Cancer diagnosis in histopathological image: CNN based approach

Sumaiya Dabeer [*], Maha Mohammed Khan, Saiful Islam

Department of Computer Engineering Zakir Husain College of Engineering and Technology Aligarh, India

ARTICLE INFO

ABSTRACT

Breast cancer affects one out of eight females worldwide. It is diagnosed by detecting the malignancy of the cells of breast tissue. Modern medical image processing techniques work on histopathology images captured by a microscope, and then analyze them by using different algorithms and methods. Machine learning algorithms are now being used for processing medical imagery and pathological tools. Manual detection of a cancer cell is a tiresome task and involves human error, and hence computer-aided mechanisms are applied to obtain better results as compared with manual pathological detection systems. In deep learning, this is generally done by extracting features through a convolutional neural network (CNN) and then classifying using a fully connected network. Deep learning is extensively utilized in the medical imaging field, as it does not require prior expertise in a related field. In this paper, we have trained a convolutional neural network and obtained a prediction accuracy of up to 99.86%.

1. Introduction

Among all types of cancer in women, breast cancer is most likely to occur. Breast cancer has the second highest mortality rate after Lung & Bronchial cancer, and about 30% of newly diagnosed cases are of breast cancer only [1]. Advancing the fight against cancer requires early detection which can only be possible with an efficient detection system. Techniques have been developed to detect breast cancer, including medical image processing and digital pathology [2–6]. Images are acquired by histopathology, which generally includes biopsy of the affected tissue. Tissues affected by the tumor are extracted by the pathologist and stained by H& E, which is the combination of histological stains called hematoxylin and eosin, after which it is examined under a microscope for cancerous cells by finding malignant features in cellular structures such as nuclei. These microscopic images can be collected and used for developing computer-aided detection systems. Manual detection is a tedious, tiring task and most likely to comprise human error, as most parts of the cell are frequently part of irregular random and arbitrary visual angles. The goal is to identify whether a tumor is benign or of a malignant in nature, as malignant tumors are cancerous and should be treated as soon as possible to reduce and prevent further complications. In short, it is a binary classification problem and can be resolved by various machine learning methods [7]. It has

been shown in the past that machine learning algorithms perform better than a human pathologist. A majority of scholars have found that medical image processing using machine learning provides more accurate results as compared to the objective diagnosis given by a pathologist. A study in Europe has been conducted by Phillips in which a set of algorithms along with breast images provided more accurate detection [8]. This finding is also evidence that using high-resolution images and better algorithms will improve the performance and accuracy of cancer detection. The remainder of this paper is structured as follows: Section II discusses the published literature along with the BreakHis dataset [9] which is the dataset used for obtaining experimental results herein. Section III describes the preprocessing steps and architecture of the CNN used in the experiment followed by neural network classification. Results are represented in Section IV. Finally, Section V concludes the work by presenting some insights for further research.

2. Background study and related work

2.1. Literature survey

There are various ways to detect breast cancer including Mammography, Magnetic Resonance Imaging (MRI) Scans, Computed Tomography (CT) Scans, Ultrasound, and Nuclear Imaging. Although, none of

---

* Corresponding author.
E-mail addresses: sumaiyadabeer@zhcet.ac.in (S. Dabeer), mahak.2j@gmail.com (M.M. Khan), saifulislam@zhcet.ac.in (S. Islam).

Table 1
Distribution of images in dataset.

Magnification	Benign	Malignant	Total
40x	652	1370	1995
100x	644	1437	2081
200x	623	1390	2013
400x	588	1232	1820
Total	2480	5429	7909

these aforementioned techniques gives a completely correct prediction of cancer. Tissue-based diagnosis is mainly done with a staining methodology. In this procedure elements of tissues are colored by some staining element, usually hematoxylin and eosin (H&E). Cell structures, types, and other foreign elements are stained accordingly, and are easily visible under high resolution. Pathologists then examine the slide of stained tissues under a microscope or using high-resolution images taken from the camera. For detection of tumors, a histopathology test is essential. It is an old method used to predict invasive cancer cells from H&E stained tissues. There are various shortcomings for this procedure as it involves intra-observer variation, cancer cells and tissues can also have multiple appearances, and many other figures in cells have the same hyperchromatic features, which make identification difficult. The choice of area is also a factor as the process is done only on a small area of tissue, so the chosen area should be in the tumor periphery. The above-mentioned problems can be addressed by using deep learning strategies. Deep learning is a popular subset of machine learning technology which is inspired by the working of the human brain to analyze unstructured patterns. Deep learning models have a high success rate because they train on hierarchical representations. Moreover, they can extract and organize different features and hence do not require any prior domain knowledge. On the other hand, trivial methods need rigorous feature engineering to obtain features, which involves domain expertise. Many deep learning methods have been proposed to predict the class of tumor. Most of them are binary classification [2,3] but some of them have used multivariable classification [10]. Deep learning algorithms only need the data in the proper format and some network parameters appropriate to the problem. One can also use predesigned networks such as AlexNet, MobileNet, Inception, and many more [11].

There are various methods and manual networks proposed by various scholars to classify breast cancer other than the predesigned networks stated above. For example, Artificial Neural Networks depend upon MLE (Maximum Likelihood Estimation) [4]. RBF Neural Networks are used in paper [12], the GRU-SVM model which is the ML algorithm combined with a type of recurrent neural network (RNN) and gated recurrent unit (GRU) with the support vector machine (SVM) [5]. Along with these techniques, other scholars have developed methodology to obtain better results with less computational complexity. For reducing the input feature size, Karabatak et al. proposed the AR + NN method, in which the number of features are reduced by applying association rules [13]. A combination of NN and multivariate adaptive regression splines (MARS) are also utilized to detect cancer [14]. There is another system that consists of the fuzzy-artificial immune system and the K-NN algorithm described in Ref. [6]. Descriptors such as CLBP, GLCM, LBP, LPQ, ORB, PFTAS are defined in paper [9] with classification of breast cancer up to a maximum accuracy of 85.1%. As for the BreakHis dataset published in 2015, only some scholars have used this. For example, Fabio A. Spanhol [3] describes parameters and the network setup which has obtained an accuracy ranging from 80 to 85%. This is further enhanced by the proposed method described herein. Moreover, in the Discussion section we present a summary of other methods along with their accuracies. In deep learning algorithms, a series of tasks are implemented. The first step is image preprocessing which is required to convert data into the format in which it can directly be input to the network. This step involves multiple channeling of images, then segmentation [15] is done (only if required, e.g. if there is a need to separate regions of interest from the background or omit parts that are not needed for training). On this stage, data is ready to be used in training, either in a supervised or an unsupervised manner. The next step is feature extraction. Features represent the visual content of the histopathology image. In the case of supervised feature extraction, features are known and different strategies are applied to find them [16–18], but in case of unsupervised feature extraction methods, features are not known and acquired implicitly in proposed solutions through the Convolutional Neural Network (CNN). The last step is classification, which places an image into the respective class (benign or malignant) and can be done using SVM (support vector machine) or with a fully connected layer using an activation function such as Softmax.

2.2. Dataset used

There are various datasets which are available for histopathological stained images like Breast Cancer for breast (WDBC) cancer Wisconsin Original Data Set (UC Irvine Machine Learning Repository) [19], MITOS- ATYPIA-14 [20] and BreakHis [9]. We have utilized the BreakHis database, which has been accumulated from the result of a survey by P&D Lab, Brazil during the span of January 2014 to December 2014. Breast tissues are taken as samples by the procedure of surgical (open) biopsy (SOB). Samples are stained by hematoxylin and eosin and produced by a standard paraffin process in which specimen infiltration and embedment are done in paraffin. Images are taken by a Samsung high-resolution device (SCC-131AN) which is coupled with an Olympus BX-50 microscopic system equipped with a relay lens with a magnification of $3.3\times$. These histopathology images have a RGB (three channel) TrueColor (8 bits- Red, 8 bits- Green, 8 bits- Blue) color coding scheme. This database contains a total of 7009 images of 700×460 pixel resolution. Images are captured in four different magnification levels. The distribution of images is summarized in Table 1.

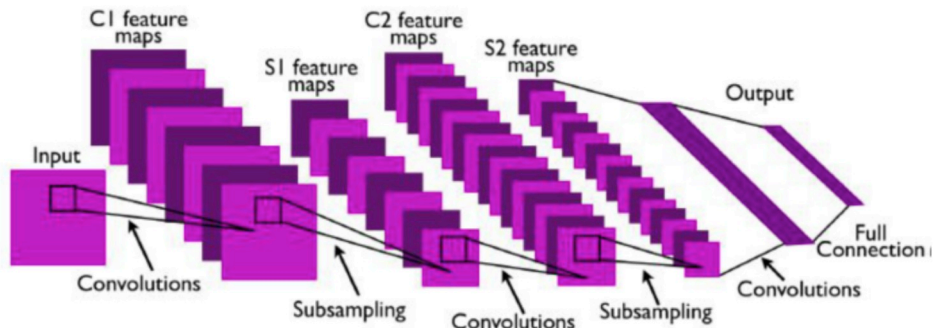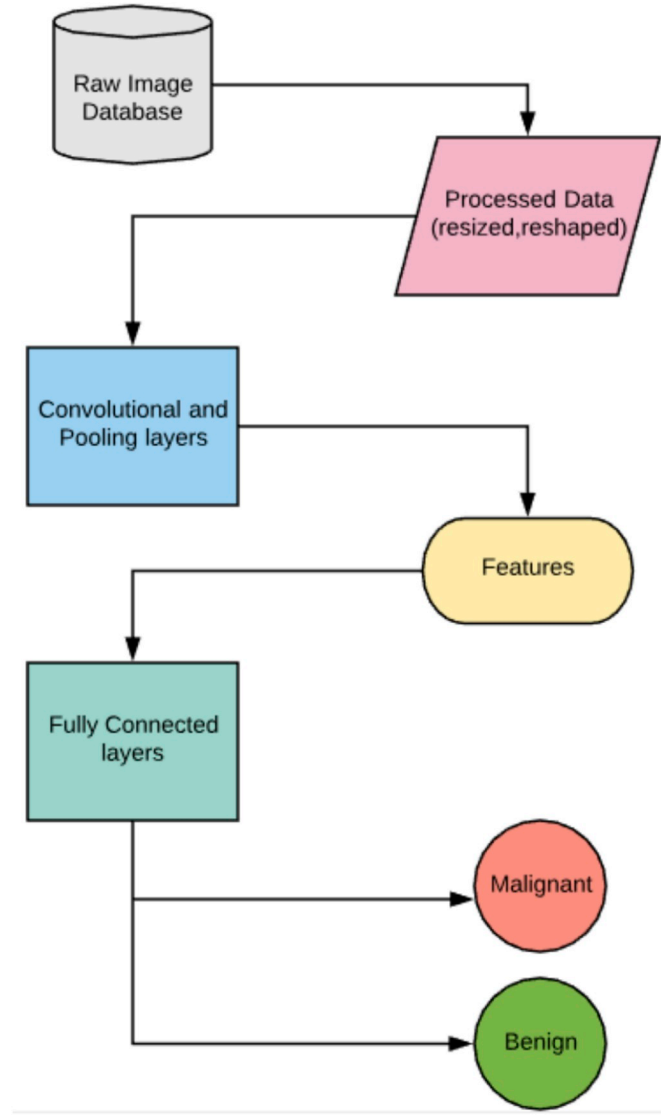**Fig. 1.** CNN architecture [26].

Fig. 2. Dataflow diagram of proposed method.

Table 2
Parameters of the CNN architecture.

Layer attribute	L1	L2	L3	L4	L5	L6
Type	conv	pool	conv	pool	conv	pool
Channel	32	–	64	–	128	–
Filter Size	5×5	–	5×5	–	5×5	–
Conv. stride	1×1	–	1×1	–	1×1	–
Pooling size	–	3×3	–	3×3	–	3×3
Pooling stride	–	1×1	–	1×1	–	1×1
Padding size	same	none	–	none	–	none
Activation	ReLu	–	ReLu	–	ReLu	–

2.3. Convolutional neural network

CNN is a modified variety of deep neural net which depends upon the correlation of neighboring pixels. It uses randomly defined patches for input at the start, and modifies them in the training process. Once training is done, the network uses these modified patches to predict and

validate the result in the testing and validation process. Convolutional neural networks [21] have achieved success in the image classification problem, as the defined nature of CNN matches the data point distribution in the image. As a result, many image processing tasks adapt CNN for automatic feature extraction. CNN is frequently used for image segmentation [22–24] and medical image processing [25] as well.

The CNN architecture has two main types of transformation. The first is convolution, in which pixels are convolved with a filter or kernel. This step provides the dot product between image patch and kernel. The width and height of filters can be set according to the network, and the depth of the filter is the same as the depth of the input. A second important transformation is subsampling, which can be of many types (max_pooling, min_pooling and average_pooling) and used as per requirement. The size of the pooling filter can be set by the user and is generally taken in odd numbers. The pooling layer is responsible to lower the dimensionality of the data, and is quite useful to reduce overfitting. After using a combination of convolution and pooling layers, the output can be fed to a fully connected layer for efficient classification. The visualization of the entire process is presented in Fig. 1.

Apart from the architecture of CNN, there is an additional key point, i.e., that simplicity to the user is helpful on the development side, as CNN requires a tremendous amount of data for training. It also requires more training time as compared to other supervised and unsupervised training approaches.

3. Proposed method

This paper introduces and assesses a deep learning architecture for automized breast cancer detection that incorporates concepts of machine learning and image classification. We have described different Deep Neural Network architectures, especially those adapted to image data such as Convolutional Neural Networks. This used the labeled (benign/malignant) input image from the raw pixels and highlighted the visual patterns, and then utilize those patterns to distinguish between non-cancerous and cancer containing tissue, working akin to digital staining, which spotlights image segments crucial for diagnostic decisions, with the help of a classifier network. The CNN was trained using 2480 benign and 5429 malignant samples belonging to the RGB color model. Therefore, the proposed system depicted in Fig. 2 provides an effective classification model for classifying breast tissue as being either benign or malignant.

3.1. Image preprocessing

Most of the pixels in the image are redundant and do not contribute substantially to the intrinsic information of an image [27]. While dealing with AI networks, it is required to eliminate them to avoid unnecessary computational overhead. This can be achieved by compression techniques. We begin the implementation of our deep net by processing the images in the dataset. This is achieved with the help of the OpenCV library in Python. There are many other modules that can be used in this step e.g. MATLAB or other image processing libraries or software. This is necessary to remove redundancy from the input data which only contributes to the computational complexity of the network without providing any significant improvements in the result. The aspect ratio of the original slide is preserved since both the dimensions are reduced by a factor of 2, giving an image which is 1/4th in area, that is of dimension 350×230 pixels.

3.2. Feature extraction

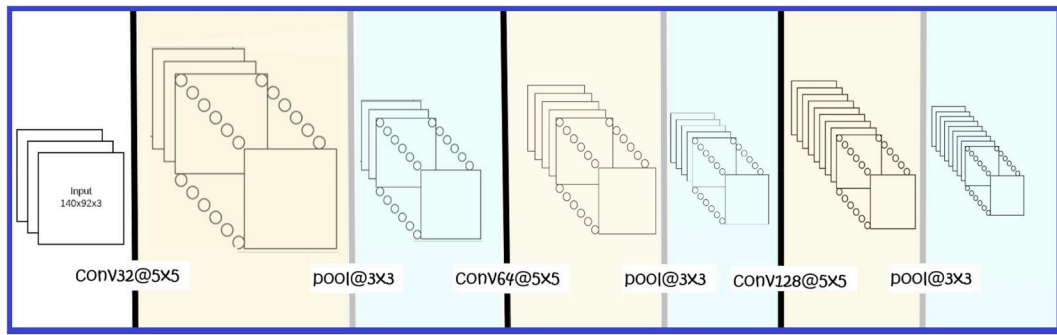Feature learning is a crucial step in the classification process for both

Fig. 3. Visual representation of layers in the convolution process.

Table 3
Details of fully connected network.

Layer Attribute	FC-1	FC-2	FC-3
No of nodes	64	64	2
Activation used	ReLu	ReLu	Softmax

Table 4
Summary of result.

	Precision	Recall	F1-score
Benign	0.91	0.88	0.89
Malignant	0.95	0.96	0.95
Avg/total	0.93	0.93	0.93

cytoplasm to nucleus decreases [29]. All of these features are examined by experts, or algorithms are developed to quantify these features to automate detection. This approach is difficult and imprecise as selection and quantification involve various unknown errors that are hard to address. In the case of supervise learning, we do not need to provide these features explicitly. In this case images are fed to an architecture such as CNN, along with its class as a label (Benign or Malignant). From the automatic update of filter values in the training process, CNN is able to extract the computational features. In short, for a given architecture of CNN filters and their weights, are features that are used at the time of testing for model evaluation. In this approach, CNN takes raw pixels of an image and gives output as learned filter weights. These weights serve input to the dense architecture of the deep neural network for final prediction. In our proposed architecture, the convolutional neural network is made up of two types of layers:

- Convolutional Layers
- Pooling Layers

The details of the network are illustrated in Table 2, followed by its visual representation in Fig. 3.

When the convolution process is done, the depth of input is increased by the number of filters used, and when the pooling layer is applied, depth remains the same and size is reduced. Visual representation of
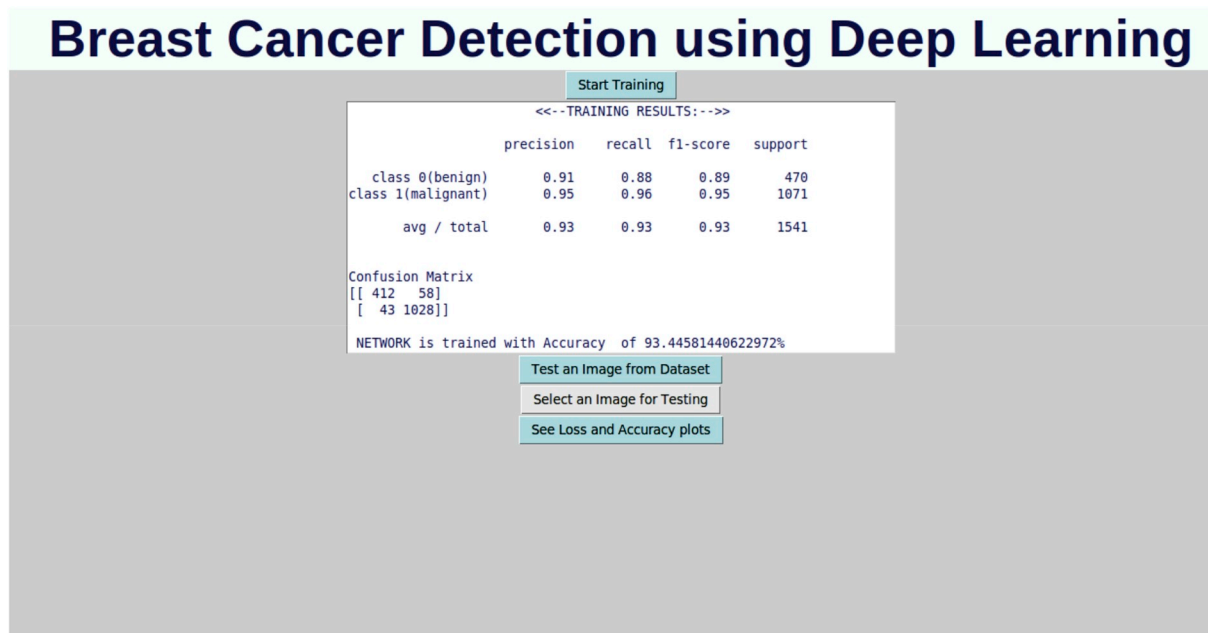
human and machine algorithm. A study has shown that the human brain is sensitive to shapes, while computers are more sensitive to patterns and texture, [28]. Because of this fact, feature learning is entirely different for manual versus machine. In the visual context, malignant tumors tend to have large and irregular nuclei or multiple nuclear structures. The cytoplasm also undergoes changes, wherein new structures appear, or normal structures disappear. Malignant cells have a small cytoplasmic amount, frequently with vacuoles. In this scenario, the ratio of

Fig. 4. Graphical user interface.

Fig. 5. Confusion matrix.

Table 2 is shown in Fig. 3 convX@Y×Y represents convolution with X number of filters of size Y×Y, and pool@Z×Z represents max pooling with a kernel size of Z×Z.

3.3. Classification

The process of classification is done by taking the flattened weighted feature map obtained from the final pooling layer, and is used as input to the fully connected network, which calculates the loss and modifies the weights of the internal hidden nodes accordingly. The parameters of these layers can be found in Table 3.

These layers are stacked after preprocessing is done. The output of the last layer is taken as the final output as usual.

4. Experimental results

By considering the previously described setup we have obtained a training accuracy of 93.45% with a test train split of 0.2. Evaluation metrics are given in Table 4 and are defined as follows. Precision is a probabilistic measure to determine whether a positive case, defined on our terms, actually belongs to the positive class. A recall is a probabilistic measure to determine if an actual positive case is correctly classified with the positive class. The F1 score is calculated as the geometric mean between precision and recall [30].

$$F1 = 2(\text{precision} * \text{recall}) / (\text{precision} + \text{recall}) \quad (1)$$

Support is the number of samples of the true response that resides in that class. The results can be summarized into Table 4, from which we can see that precision for the benign and malignant classes are found to be 90.55% and 94.66%, respectively. Moreover, the recall for two classes are 87.66% and 95.98% respectively.

Confusion matrix obtained in this experiment is given in Fig. 5 which graphically summarizes the result of Table 4. From Fig. 5 we can conclude that the Malignant class is the true class in this case; hence values of TP, TN, FP and FN are 66.71%, 2.79%, 3.76% and 26.74%.

We have used 7909 biopsy images of benign and malignant breast tissue in this model with a train-test split of 0.2 and obtained the desired result. The predictive output of four benign and four malignant images from the testing set are displayed in Fig. 6 and Fig. 7 for demonstration purposes. Predictive confidences are listed in Table 6 for these images. These images can be found in the dataset with the name given in Table 5.

Loss and accuracy curves of training and validation obtained during the training process are displayed in Fig. 8 and Fig. 9, respectively.

As expected for a network, both losses shown in Fig. 8 start with a high value and decrease while training proceeds. This behavior is similar to the standard training procedure for deep learning. The difference in saturation levels of Training Loss and Validation Loss is 0.2, which is within the permissible range for a network to avoid underfitting or overfitting.

The graphical plot of accuracy distribution is presented in Fig. 9. Accuracy starts to increase with the number of epochs, and ultimately saturates, which shows that the training on the dataset is completed for the designed network. Moreover, an important conclusion from this graph is that the network is trained without having characteristics of underfitting and overfitting, as validation accuracy and training accuracy curves are similar in distribution.

5. Discussion

From the setup stated above, we obtained a level of accuracy which was improved over many state-of-the-art experimental setups. For comparison, we have compared our result (93.45% validation accuracy from test set)with several published studies shown in Table 7. Along with the improvement in accuracy, there is a significant improvement in precision (as 93% in our case and 63.36% [31] and 90.63% [32]) and recall (as 93% in our case and 76.67% [31] and 86.39% [32]) This approach is very useful as this system is fully automated and any user can test a new image just by selecting it using our GUI based implementation, which is shown in Fig. 4. Even at the design stage, there is no need for domain insight as our method provides a high prediction accuracy. We have tested our model with various resolution of histopathology images and the results are relatively insensitive to resolution (refer to Table 6). By using this automated process there is a possibility of inexpensive detection of cancer in the early stages, which can ultimately increase survival rate among breast cancer patients.

6. Conclusion and future scope

Breast cancer detection by using digital/digitized histopathology images is a milestone in the field of medical pathology. It has also opened a door to new opportunities for research as there are many undiscovered areas that can be revealed by techniques and tools of machine learning and deep learning. We may obtain improved results by altering the network design and parameters. As an improvement to the proposed method, one can implement an autoencoder instead of manually reducing image size. It can compress data without losing the prominent features, because autoencoders can regenerate up to 90% of the original image [34] From the point of method improvement, we can incorporate spectral imaging. Spectral imaging [35] is used to obtain images with various wavelengths, which is different from the trivial three channel RGB image. Additionally, we may combine various

(a) B40

(b) B100

(c) B200

(d) B400
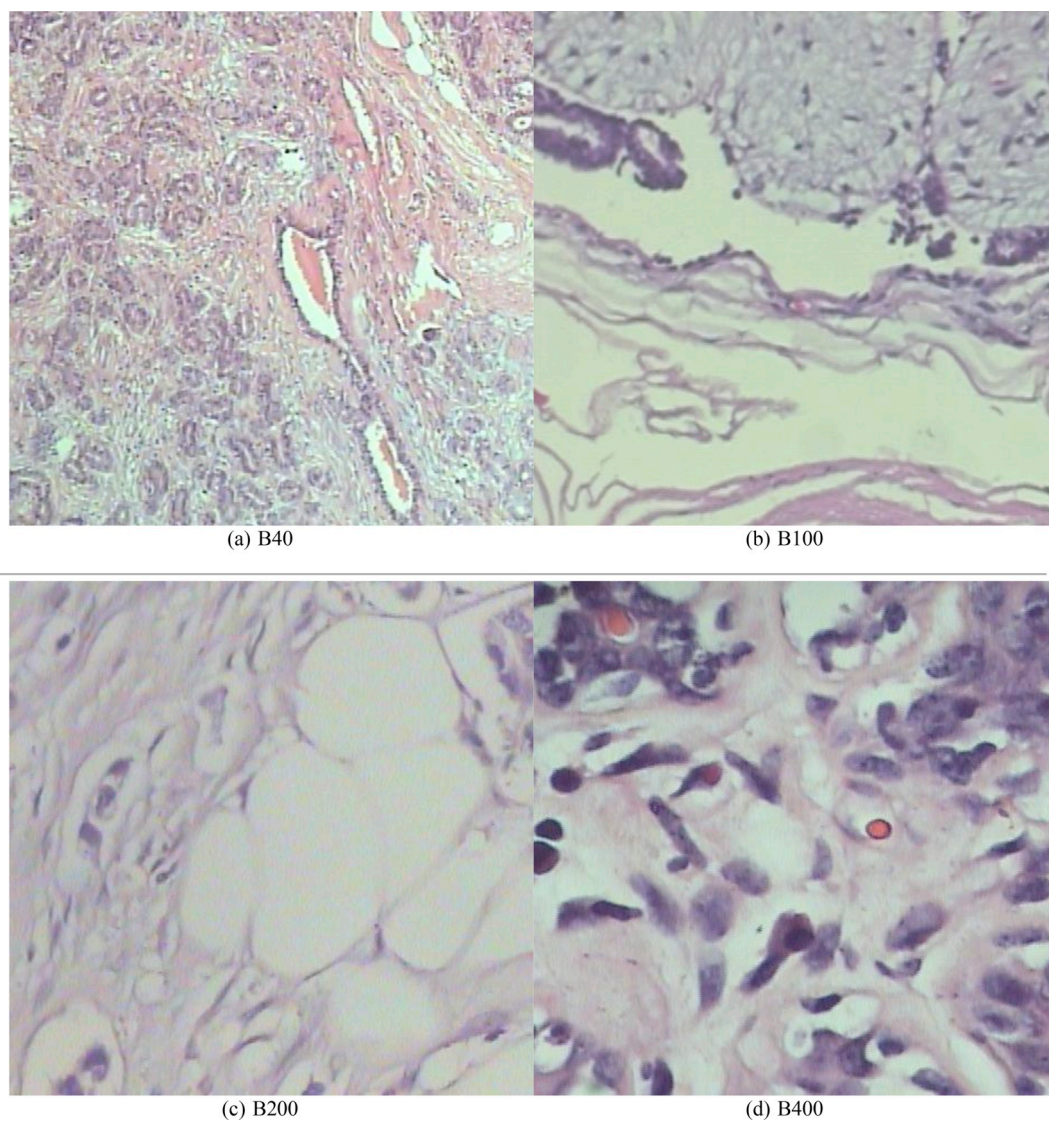
Fig. 6. Sample Benign image for Testing.

(a) M40   (b) M100

(c) M200   (d) M400
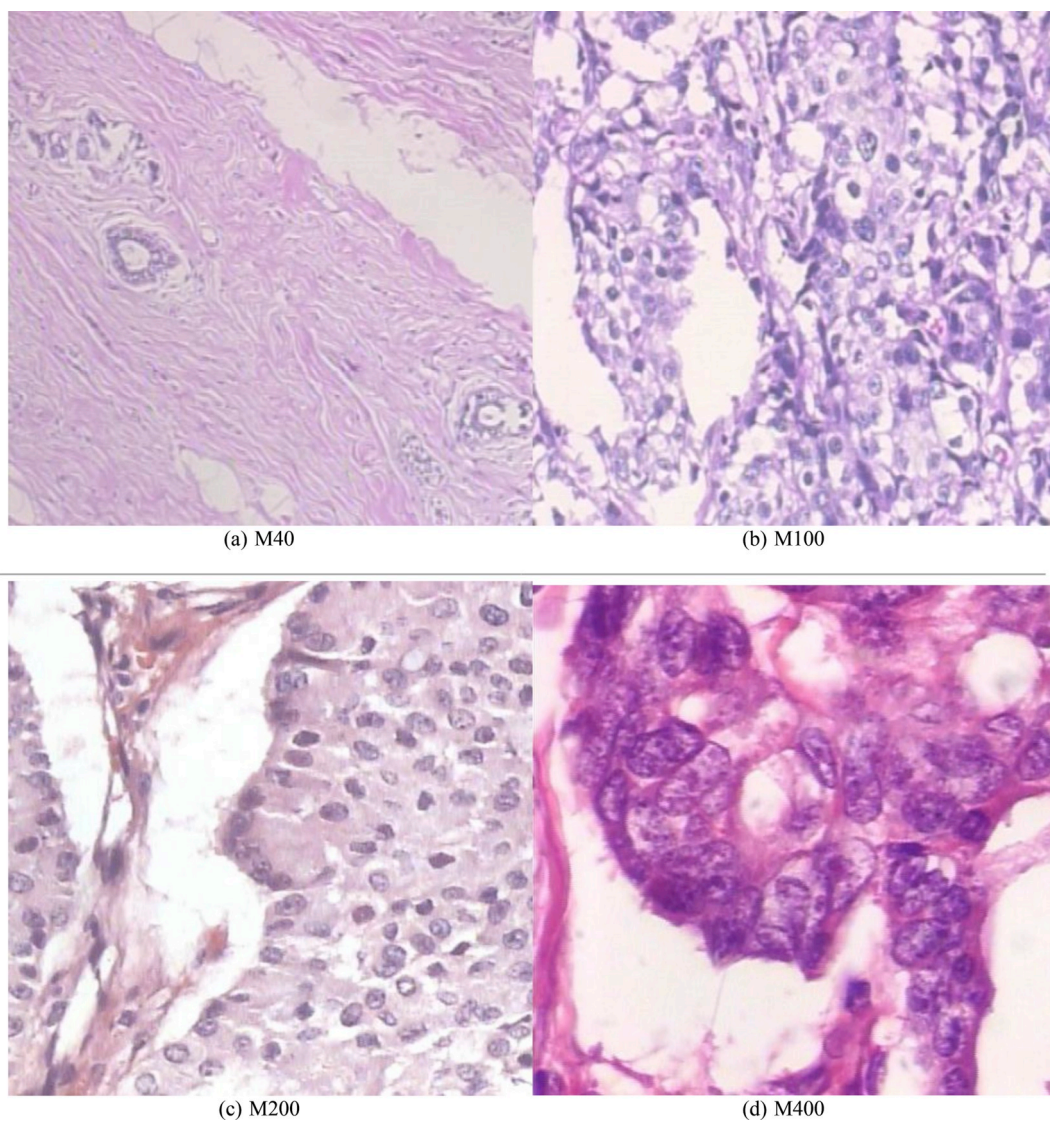
Fig. 7. Sample Malignant image for Testing.

Table 5
Details of sample images from test set.

Label	Resolution	Image name in Dataset
B40	40X	SOB_B_A-14-29960CD-40-015.png
B100	100X	SOB_B_PT-14-22704-100-018.png
B200	200X	SOB_B_TA-14-19854C-200-016.png
B400	400X	SOB_B_TA-14-13200-400-008.png
M40	40X	SOB_M_LC-14-12204-40-001.png
M100	100X	SOB_M_LC-14-12204-100-049.png
M200	200X	SOB_M_MC-14-13418DE-200-012.png
M400	400X	SOB_M_PC-14-12465-400-013.png

Table 6
Prediction result.

Label	Actual Class	Predicted Accuracy	Predicted Class
B40	Benign	100%	Benign
B100	Benign	99.99%	Benign
B200	Benign	99.99%	Benign
B400	Benign	99.99%	Benign
M40	Malignant	100%	Malignant
M100	Malignant	99.99%	Malignant
M200	Malignant	99.99%	Malignant
M400	Malignant	99.99%	Malignant

Fig. 8. Training loss and validation loss.
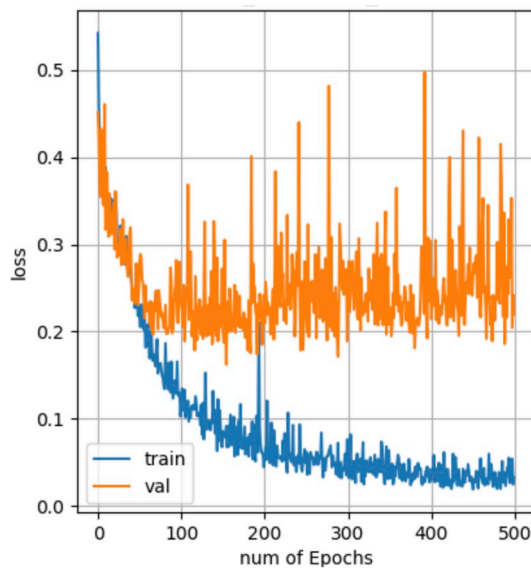
imaging technologies such as MRI, CT Scan, ultrasound, and mammographic images, and determine their collective results. This technique is known as multimodel fusion [36,37]. Problems stated above can again readily be solved by deep learning, and can be used to perform high quality research that might provide even better results.
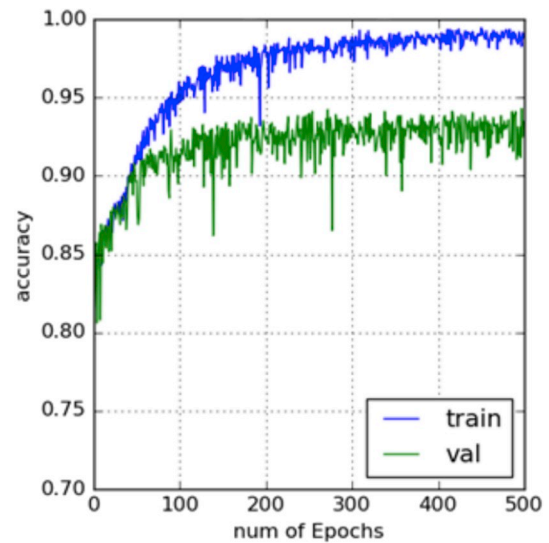

Fig. 9. Training accuracy and validation accuracy.

Table 7
Existing methods and respective Accuracy.

Year	Method Used	Validation Accuracy Range (in %)	Error Rate
2017	K-Nearest Neighbor [32]	83 to 86	19.28
2017	Pre-Trained Networks [11]	80 to 89	4.74
2017	Feature Extracted Using CNN [33]	83 to 90	4.28
2018	Deep Convolution Neural Network [31]	91.54	8.54

Appendix A. Supplementary data

Supplementary data to this article can be found online at https://doi.org/10.1016/j.imu.2019.100231.

References

[1] Siegel RL, Miller KD, Jemal A. Cancer statistics, 2017. CA - Cancer J Clin 2017;67(1):7–30.

[2] Spanhol FA, Oliveira LS, Cavalin PR, Petitjean C, Heutte L. Deep features for breast cancer histopathological image classification. In: 2017 IEEE international conference on systems, man, and cybernetics, SMC 2017, banff, AB, Canada, october 5-8, 2017; 2017. p. 1868–73. https://doi.org/10.1109/SMC.2017.8122889. https://doi.org/10.1109/SMC.2017.8122889.

[3] Spanhol FA, Oliveira LS, Petitjean C, Heutte L. Breast cancer histopathological image classification using convolutional neural networks. In: 2016 international joint conference on neural networks, IJCNN 2016, vancouver, BC, Canada, july 24-29, 2016; 2016. p. 2560–7. https://doi.org/10.1109/IJCNN.2016.7727519. https://doi.org/10.1109/IJCNN.2016.7727519.

[4] A. Alias, B. Paulchamy, Detection of breast cancer using artifical neural network, International Journal of Innovative Research in Science 3 (3).

[5] Agarap AF. On breast cancer detection: an application of machine learning algorithms on the Wisconsin diagnostic dataset, CoRR abs/1711.07831. 1711.07831. http://arxiv.org/abs/1711.07831.

[6] Sahan S, Polat K, Kodaz H, Günes S. A new hybrid method based on fuzzy-artificial immune system and k-nn algorithm for breast cancer diagnosis. Comput Biol Med 2007;37(3):415–23. https://doi.org/10.1016/j.compbiomed.2006.05.003. https://doi.org/10.1016/j.compbiomed.2006.05.003.

[7] R. A. Johnson, D. W. Wichern, Multivariate analysis, Encyclopedia of Statistical Sciences 8.

[8] Lowe A KMe a, Grunkin M. Visiopharm digital pathology blog philips teams up with visiopharm to boost breast cancer diagnosis objectivity through computational pathology. 2016. http://www.visiopharm.com/blog/category/image-_analysis/.

[9] Spanhol FA, Oliveira LS, Petitjean C, Heutte L. A dataset for breast cancer histopathological image classification. IEEE Trans Biomed Eng 2016;63(7): 1455–62. https://doi.org/10.1109/TBME.2015.2496264. https://doi.org/10.110 9/TBME.2015.2496264.

[10] Han Z, Wei B, Zheng Y, Yin Y, Li K, Li S. Breast cancer multi-classification from histopathological images with structured deep learning model. Sci Rep 2017;7(1): 4172.

[11] Sun J, Binder A. Comparison of deep learning architectures for h&e histopathology images. In: 2017 IEEE conference on big data and analytics (ICBDA). IEEE; 2017. p. 43–8.

[12] Kanojia MG, Abraham S. Breast cancer detection using rbf neural network. In: Contemporary computing and informatics (IC3I), 2016 2nd international conference on. IEEE; 2016. p. 363–8.

[13] Karabatak M, Ince MC. An expert system for detection of breast cancer based on association rules and neural network. Expert Syst Appl 2009;36(2):3465–9. https://doi.org/10.1016/j.eswa.2008.02.064. https://doi.org/10.1016/j.eswa.200 8.02.064.

[14] Chou S, Lee T, Shao YE, Chen I. Mining the breast cancer pattern using artificial neural networks and multivariate adaptive regression splines. Expert Syst Appl 2004;27(1):133–42. https://doi.org/10.1016/j.eswa. 2003.12.013. https://doi.org/10.1016/j.eswa.2003.12.013.

[15] A. Chon, N. Balachandra, P. Lu, Deep convolutional neural networks for lung cancer detection, Standford University.

[16] Cruz-Roa AA, Ovalle JEA, Madabhushi A, Osorio FAG. A deep learning architecture for image representation, visual interpretability and automated basal-cell carcinoma cancer detection. In: Medical image computing and computer-assisted intervention - (MICCAI) 2013 - 16th international conference, nagoya, Japan, september 22-26, 2013, proceedings, Part II; 2013. p. 403–10. https://doi.org/10.1007/978-_3-_642-_ 40763-_5_50. https://doi.org/10.1007/978-3-642-4 0763-5_50.

[17] Veta M, van Diest PJ, Willems SM, Wang H, Madabhushi A, Cruz-Roa A, González FA, Larsen ABL, Vestergaard JS, Dahl AB, Ciresan DC, Schmidhuber J, Giusti A, Gambardella LM, Tek FB, Walter T, Wang C, Kondo S, Matuszewski BJ, Precioso F, Snell V, Kittler J, de Campos TE, Khan AM, Rajpoot NM, Arkoumani E, Lacle MM, Viergever MA, Pluim JPW. Assessment of algorithms for mitosis detection in breast cancer histopathology images. Med Image Anal 2015;20(1): 237–48. https://doi.org/10.1016/j.media.2014.11.010. https://doi.org/10.1016/j.media.2014.11.010.

[18] Kumar R, Srivastava R, Srivastava S. Detection and classification of cancer from microscopic biopsy images using clinically significant and biologically interpretable features. Journal of medical engineering 2015. https://doi.org/10.1155/2015/457906. https://doi.org/10.1155/2015/457906.

[19] W. H. Wolberg, W. N. Street, O. L. Mangasarian, Breast cancer Wisconsin (diagnostic) data set, UCI Machine Learning Repository [http://archive.ics.uci.edu/ml/].

[20] Lowe A KMe a, Grunkin M. Mitos atypia grand challenge 2014. 2014. https://mitos-_atypia-_14.grand-_challenge.org/Dataset/.

[21] LeCun Y, Bengio Y, Hinton G. Deep learning, nature 2015;521(7553):436. https://doi.org/10.1038/nature14539. https://doi.org/10.1038/nature14539.

[22] Xing F, Xie Y, Yang L. An automatic learning-based framework for robust nucleus segmentation. IEEE Trans Med Imaging 2016;35(2):550–66. https://doi.org/10.1109/TMI.2015.2481436. https://doi.org/10.1109/TMI.2015.2481436.

[23] Prasoon A, Petersen K, Igel C, Lauze F, Dam E, Nielsen M. Deep feature learning for knee cartilage segmentation using a triplanar convolutional neural network. In: Medical image computing and computer-assisted intervention - (MICCAI) 2013 - 16th international conference, nagoya, Japan, september 22-26, 2013, proceedings, Part II; 2013. p. 246–53. https://doi.org/10.1007/978-_3-_642-_ 40763-_5_31. https://doi.org/10.1007/978-3-642-40763-5_31.

[24] Ciresan DC, Giusti A, Gambardella LM, Schmidhuber J. Deep neural networks segment neuronal membranes in electron microscopy images. In: Advances in neural information processing systems 25: 26th annual conference on neural information processing systems 2012. Proceedings of a meeting held december 3-6, 2012, lake tahoe, Nevada, United States.; 2012. p. 2852–60.

[25] Cruz-Roa A, Basavanhally A, González FA, Gilmore H, Feldman M, Ganesan S, Shih N, Tomaszewski J, Madabhushi A. Automatic detection of invasive ductal carcinoma in whole slide images with convolutional neural networks. In: Medical imaging 2014: digital pathology, san diego, California, United States, 15-20 february 2014; 2014. p. 904103. https://doi.org/10.1117/12.2043872. https://doi.org/10.1117/12.2043872.

[26] Krizhevsky A, Sutskever I, Hinton GE. Imagenet classification with deep convolutional neural networks. Commun ACM 2017;60(6):84–90. https://doi.org/10.1145/3065386. https://doi.org/10.1145/3065386.

[27] González RC, Woods RE, Eddins SL. Digital image processing using MATLAB. Pearson; 2004.

[28] Geirhos R, Rubisch P, Michaelis C, Bethge M, Wichmann FA, Brendel W. Imagenet-trained CNNs are biased towards texture; increasing shape bias improves accuracy and robustness. In: International conference on learning representations; 2019. https://openreview.net/forum?id=Bygh9j09KX.

[29] Baba AI, Cătoi C. Tumor cell morphology. In: Comparative oncology. The Publishing House of the Romanian Academy; 2007.

[30] Sokolova M, Japkowicz N, Szpakowicz S. Beyond accuracy, f-score and ROC: a family of discriminant measures for performance evaluation. In: AI 2006: advances in artificial intelligence, 19th Australian joint conference on artificial intelligence, hobart, Australia, december 4-8, 2006, proceedings; 2006. p. 1015–21. https://doi.org/10.1007/11941439_114. https://doi.org/10.1007/11941439%5c_114.

[31] Adeshina SA, Adedigba AP, Adeniyi AA, Aibinu AM. Breast cancer histopathology image classification with deep convolutional neural networks. In: 2018 14th international conference on electronics computer and computation (ICECCO). IEEE; 2018. p. 206–12.

[32] Samah AA, Fauzi MFA, Mansor S. Classification of benign and malignant tumors in histopathology images. In: 2017 IEEE international conference on signal and image processing applications, ICSIPA 2017, kuching, Malaysia, september 12-14, 2017; 2017. p. 102–6. https://doi.org/10.1109/ICSIPA.2017.8120587. https://doi.org/1 0.1109/ICSIPA.2017.8120587.

[33] Song Y, Zou JJ, Chang H, Cai W. Adapting Fisher vectors for histopathology image classification. In: 14th IEEE international symposium on biomedical imaging, ISBI 2017, melbourne, Australia, april 18-21, 2017; 2017. p. 600–3. https://doi.org/10.1109/ISBI.2017.7950592. https://doi.org/10.1109/ISBI.2017.7950592.

[34] Ng A, et al. Sparse autoencoder, CS294A Lecture notes, vol. 72; 2011. p. 1–19. 2011.

[35] Sattar A, Kang BH, editors. AI 2006: advances in artificial intelligence, 19th Australian joint conference on artificial intelligence, hobart, Australia, december 4-8, 2006, proceedings, vol. 4304 of lecture notes in computer science. Springer; 2006. https://doi.org/10.1007/11941439. https://doi.org/10.1007/11941439.

[36] Anshad PM, Kumar S. Recent methods for the detection of tumor using computer aided diagnosisa review. In: Control, instrumentation, communication and computational technologies (ICCICCT), 2014 international conference on. IEEE; 2014. p. 1014–9.

[37] El-Gamal FE-ZA, Elmogy M, Atwan A. Current trends in medical image registration and fusion. Egyptian Informatics Journal 2016;17(1):99–124.

Update

Informatics in Medicine Unlocked
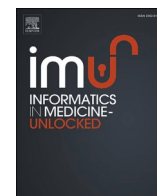
Erratum regarding missing Declaration of Competing Interest statements in previously published articles

Declaration of Competing Interest statements were not included in published version of the articles that appeared in previous volumes of Informatics in Medicine Unlocked. Hence, the authors of the below articles were contacted after publication to request a Declaration of Interest statement:

1. "Automated scraping of structured data records from health discussion forums using semantic analysis" [Informatics in Medicine Unlocked, 2018; 10C: Pages: 149–158] https://doi.org/10.1016/j.imu.2018.01.003

2. "Molecular dynamics simulation approach to explore atomistic molecular mechanism of peroxidase activity of apoptotic cytochrome c mutants" [Informatics in Medicine Unlocked, 2018; 11C; Pages: 51–60] https://doi.org/10.1016/j.imu.2018.04.003

3. "An efficient and secure remote user mutual authentication scheme using smart cards for Telecare medical information systems" [Informatics in Medicine Unlocked, 2018; 16C: Article Number: 100092] https://doi.org/10.1016/j.imu.2018.02.003

4. "A numerical modelling of an amperometric-enzymatic based uric acid biosensor for GOUT arthritis diseases" [Informatics in Medicine Unlocked, 2019; 12C: Pages: 143–147] https://doi.org/10.1016/j.imu.2018.03.001

5. "Automated heartbeat classification and detection of arrhythmia using optimal orthogonal wavelet filters" [Informatics in Medicine Unlocked, 2019, 16C; Article number: 100221] https://doi.org/10.1016/j.imu.2019.100221

6. "CHROMATOGRAPHIC ANALYSIS OF PHYTOCHEMICALS IN COSTUS IGNEUS AND COMPUTATIONAL STUDIES OF FLAVONOIDS" [Informatics in Medicine Unlocked, 2018; 13C: page range: 34–40] https://doi.org/10.1016/j.imu.2018.10.004

7. "Sperm motility analysis system implemented on a hybrid architecture to produce an intelligent analyzer" [Informatics in Medicine Unlocked, 2020; 19C; Article number: 100324] https://doi.org/10.1016/j.imu.2020.100324

8. "Medical video compression using bandelet based on lifting scheme and SPIHT coding: in search of high visual quality" [Informatics in Medicine Unlocked, 2019; 17C: Article number 100244] https://doi.org/10.1016/j.imu.2019.100244

9. "A histopathological image dataset for grading breast invasive ductal carcinomas" [Informatics in Medicine Unlocked, 2020; 19C: Article number 100341] https://doi.org/10.1016/j.imu.2020.100341

10. "Cancer diagnosis in histopathological image: CNN based approach" [Informatics in Medicine Unlocked, 2019; 16C: Article number 100231] https://doi.org/10.1016/j.imu.2019.100231

11. "The open D1NAMO dataset: A multi-modal dataset for research on non-invasive type 1 diabetes management" [Informatics in Medicine Unlocked, 2018; 13C: Pages: 92–100] https://doi.org/10.1016/j.imu.2018.09.003

12. "The prediction of good physicians for prospJective diagnosis using data mining" [Informatics in Medicine Unlocked, 2018; 12C: Pages 120–127] https://doi.org/10.1016/j.imu.2018.07.005

13. "Prediction of Pathological Complete Response after Neoadjuvant Chemotherapy for Breast Cancer using Ensemble Machine Learning" [Informatics in Medicine Unlocked, 2019; 16C: Article number: 100219] https://doi.org/10.1016/j.imu.2019.100219

14. "Classification of intra-genomic helitrons based on features extracted from different orders of FCGS" [Informatics in Medicine Unlocked, 2019; 18C: Article number: 100271] https://doi.org/10.1016/j.imu.2019.100271

15. "Visual feedback framework for rehabilitation of stroke patients" [Informatics in Medicine Unlocked, 2018; 13C: Pages: 41–50] https://doi.org/10.1016/j.imu.2018.10.002

16. "Performance of source imaging techniques of spatially extended generators of uterine activity" [Informatics in Medicine Unlocked, 2019; 16C Article number: 100167] https://doi.org/10.1016/j.imu.2019.100167

17. "Automated classification of benign and malignant cells from lung cytological images using deep convolutional neural network" [Informatics in Medicine Unlocked, 2019; Volume 16C: Article number: 100205] https://doi.org/10.1016/j.imu.2019.100205